Small-World to Fractal Transition in Complex Networks: A Renormalization Group Approach

Hernán D. Rozenfeld, Chaoming Song, and Hernán A. Makse

Levich Institute and Physics Department, City College of New York, New York, New York 10031, USA

(Received 26 September 2009; revised manuscript received 13 November 2009; published 11 January 2010)

We show that renormalization group (RG) theory applied to complex networks is useful to classify network topologies into universality classes in the space of configurations. The RG flow readily identifies a small-world–fractal transition by finding (i) a trivial stable fixed point of a complete graph, (ii) a nontrivial point of a pure fractal topology that is stable or unstable according to the amount of long-range links in the network, and (iii) another stable point of a fractal with shortcuts that exist exactly at the small-world–fractal transition. As a collateral, the RG technique explains the coexistence of the seemingly contradicting fractal and small-world phases and allows us to extract information on the distribution of shortcuts in real-world networks, a problem of importance for information flow in the system.

DOI: 10.1103/PhysRevLett.104.025701 PACS numbers: 64.60.aq, 02.70.Rr, 05.10.Cc, 05.45.Df

A generic property that is usually inherent in scale-free networks is the *small-world* feature [2]. In small-world networks, a small number of steps is required to reach a given node starting from any other node. This is expressed by the slow (logarithmic) increase of the diameter of the network, $\bar{r}$, with the total number of nodes N_0, $\bar{r} \sim \ln N_0$, where r is the shortest distance between two nodes through network links.

The small-world property has been shown to apply in many empirical studies of diverse systems. However, recent work [3–6] showed that many networks that have been found to display the small-world property, such as the WWW, are indeed fractal, indicating a power-law dependence of the distances with the network size, $\bar{r} \sim N_0^{1/d_B}$, where d_B is the fractal dimension, up to a certain length-scale before the global small-world behavior is observed. Therefore, it is not clear how it is possible that fractal scale-free networks coexist with the small-world property. This shows the need for a framework that reconciles these two seemingly contradictory aspects, fractality and the small-world property.

In this Letter, we show that renormalization group (RG) theory provides such a framework [3–6]. The main result of our work is fourfold. (1) We introduce a method that classifies networks into three universality classes according to fixed points of the RG flow. We find a stable trivial fixed point of a complete graph, a nontrivial fixed point of a fractal structure that becomes stable or unstable according to the amount of long-range links added to the network, and a third stable fixed point that exists exactly at the small-world–fractal transition consisting of a fractal with shortcuts. (2) The RG technique allows for finding the distribution of shortcuts overlaying a pure fractal topology, a technique that we test in real-world networks like the WWW and biological networks. (3) The RG identifies a second point which is associated with information flow in the system. (4) The RG analysis finds an explanation for the seemingly contradiction between the small-world effect observed at a global scale in real-world networks and the fractal behavior occurring at finite scales.

We apply the RG to complex networks using the box-covering technique [3]. The network is covered with boxes such that all nodes within a box are at a distance smaller than b [top panel of Fig. 1(a)], where the distance is the number of links along the shortest path between two nodes. Once the network is tiled, we construct the renormalized network by replacing each box with supernodes (or renormalized nodes). These supernodes are connected if there is at least one link between two nodes in their corresponding boxes. When this RG transformation, R_b, is applied to a network G_0, it leads to a new network G_b. If G_0 is self-similar [3–6], the RG leads to a structure that presents similar properties as G_0. More technically, if G_0 is a fractal

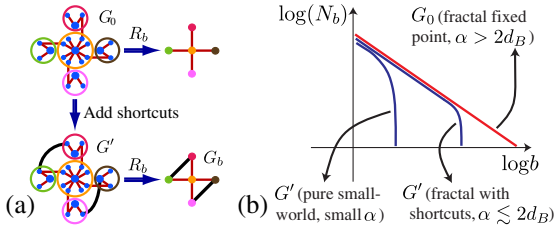

FIG. 1 (color online). (a) Top panel: fractal network G_0 with box covering for $b = 2$, and its renormalized network $R_b(G_0)$. Bottom panel: shortcuts are added (curved links in lower left panel); we obtain network G'. We apply the RG transformation to G' and obtain G_b. (b) Sketch of the number of boxes versus the box diameter according to the probability, $P(r) = Ar^{-\alpha}$, to add shortcuts between nodes at distance r. When the network is in the stable phase, $s \equiv \alpha/d_B > 2$, RG flows toward the pure fractal fixed point G_0, where the number of boxes is a power law for all values of b (straight line). When $s \lesssim 2$, the number of boxes displays a power law with an exponential cutoff at large values, indicating that globally the network topology behaves as a small world, but for small values of b the network still exhibits fractality. For small values of α, the number of boxes decays exponentially and the network displays the small-world property at all scales.

network, then $R_b(G_0) = G_0$ and G_0 is a fixed point of the RG flow.

Suppose we start with the fractal network G_0 and add shortcuts according to the distance r between nodes with probability $p(r) = Ar^{-\alpha}$, where $r > 1$. The new network with shortcuts, G', is not self-similar anymore, or in other words, $R_b(G') \neq G'$ [see Fig. 1(a)]. Here, we show that depending on the exponent α, the application of the RG process brings G' either back to the original self-similar structure G_0 or transforms it into a complete graph (where all nodes are connected to each other). G_0 and the complete graph are both *fixed points* in the space of networks. G_0 is an *unstable* fixed point of R_b since a small number of shortcuts may lead it to a different network under R_b. The complete graph is a *stable* or trivial fixed point because any small perturbation always returns the network into the complete graph under R_b.

We start by analyzing the RG flow. Let d_B be the box (or fractal) dimension of the self-similar network G_0. Thus, $b^{d_B} = N_0/N_b$ is the average number of nodes in a box of size b where N_b is the number of nodes in G_b and N_0 the number of nodes in G_0. After a renormalization step is applied to the network G', the probability to find a shortcut between two nodes at distance r in the renormalized network G_b [black links in lower right panel of Fig. 1(a)] is $p_b(r) = 1 - [1 - p(br)]^{b^{2d_B}}$, and therefore,

$$p_b(r) = 1 - [1 - A(br)^{-\alpha}]^{b^{2d_B}}. \quad (1)$$

Let $x \equiv A^{-1}(br)^{\alpha}$ and $B(r) \equiv A^{2d_B/\alpha} r^{-2d_B}$. In the limit $b \to \infty$, we find a fixed point of the RG flow defined at

$$p^*(r) \equiv \lim_{b\to\infty} p_b(r) = 1 - \left[\lim_{x\to\infty}\left(1 - \frac{1}{x}\right)^{B(r)x^{2d_B/\alpha}}\right] = 1 - \lim_{x\to\infty} \exp[-B(r)x^{2d_B/\alpha - 1}]. \quad (2)$$

Analysis of Eq. (2) reveals a critical value at $s \equiv \alpha/d_B = 2$ separating two phases of the RG flow. If $s > 2$, we find $p^*(r) = 0$. Therefore, the RG flow brings the network toward the self-similar fixed point G_0, implying that the added shortcuts disappear under the renormalization flow. If $s < 2$, we find $p^*(r) = 1$ and G' flows toward a trivial fixed point consisting of a complete graph. If $s = 2$, G' flows toward another nontrivial stable fixed point consisting of the original fractal network G_0 with shortcuts following $p^*(r) = 1 - \exp(-Ar^{-2d_B})$ [Fig. 2(a)].

To better understand the features of the phases identified by the RG flow, we analyze the behavior of the average network degree under renormalization. This calculation finds a second important point related to information flow in the system. Let z_0 and z' be the average degree (number of links per node) of G_0 and G', respectively. Then, $z' - z_0 = \frac{2M(L)}{N_0}$, where $M(L)$ is the number of shortcuts at distance L (the diameter of G_0). Since G_0 is fractal, we find

$$M(L) \approx d_B \int_1^L Ar^{-\alpha} r^{d_B - 1} dr = \frac{A}{1-s}(L^{d_B(1-s)} - 1). \quad (3)$$

Hence, we obtain

$$z' - z_0 = \frac{2A}{1-s}\left(\frac{L^{d_B(1-s)} - 1}{N_0}\right). \quad (4)$$

After renormalizing the network G' with length-scale b, shortcuts connecting nodes inside a box will not appear in the renormalized network, G_b. Therefore, the number of remaining shortcuts in G_b is simply the number of shortcuts that connect different boxes, i.e., $M(L) - M(b)$. If z_b is the average degree of G_b, then

$$z_b - z_0 = \frac{2[M(L) - M(b)]}{N_b} = (z' - z_0) f_N(b), \quad (5)$$

where

$$f_N(b) = \left(\frac{L^{d_B(1-s)} - b^{d_B(1-s)}}{L^{d_B(1-s)} - 1}\right) b^{d_B}. \quad (6)$$

Let $x_b \equiv N_0/N_b = b^{d_B}$. In the limit $L \to \infty$, we find the scaling

$$f_N(x_b) \sim x_b^{\lambda}, \quad (7)$$

where the RG exponent λ depends on the long-range exponent α as

$$\lambda = \begin{cases} 1, & \text{if } s \leq 1, \\ 2 - s, & \text{if } s > 1. \end{cases} \quad (8)$$

Equation (8) [see Fig. 2(b)] identifies two transitions separating different phases in the space of configurations, as depicted in the phase diagram of Fig. 2. The first transition at $s = 2$ corresponds to the point when $\lambda = 0$, and separates a stable phase with $\lambda < 0$ for $s > 2$ from an unstable phase with $\lambda > 0$ for $s < 2$. Therefore, this transition corresponds to the complete graph-fractal transition identified by the analysis of Eq. (2), and corresponds to the point at which the network topology dramatically changes. In the unstable phase, $s < 2$, the average degree increases ($\lambda > 0$) so that under infinite steps of the RG procedure, the network becomes a complete graph with infinite average degree in the thermodynamic limit. On the other hand, when $s > 2$, the network conserves the global fractal structure of G_0. Under the RG flow, the difference between z_b and z_0 goes to 0 and the shortcuts disappear, returning G'

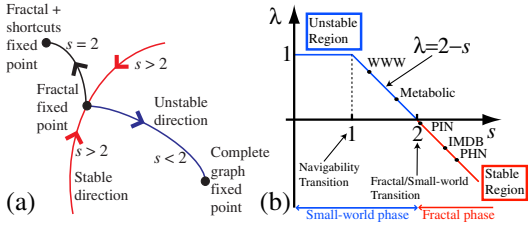

FIG. 2 (color online). (a) RG flow diagram. (b) Phase diagram of the three phases found via RG at $s < 1$, $1 < s < 2$, and $s > 2$.

back to its original fractal structure. In this state, the diameter of the network grows as a power law with the number of nodes, implying a large-world fractal structure. Instead, if long-range connections are added with $s < 2$, the small-world property is achieved, where the diameter of the network grows logarithmically with the number of nodes. Therefore, the $s = 2$ (or $\alpha = 2d_B$) transition is a small-world–fractal transition. This calculation generalizes the small/large-world transition, previously found in Refs. [8] for lattices to the case of complex networks.

As a test of the RG predictions, we use a model of fractal networks, as described in Ref. [5]. Using the fractal model, shortcuts with an exponent α can be added to the network and the prediction of Eq. (8) can be tested in a controlled manner. The fractal model network is built as follows [5]: At generation $n = 0$, we start with a star network of 5 nodes, i.e., a node in the center and four nodes connected to the center node. Then, generation $n + 1$ is obtained recursively by attaching m new nodes to the endpoints of each link l of generation n. In addition, we remove links l of generation n and add x new links connecting pairs of new nodes attached to the endpoints of l [see top panel of Fig. 1(a) for an example at with $n = 2$, $m = 2$, and $x = 1$]. The algorithm leads to a pure fractal scale-free network with degree distribution exponent $\gamma = 1 + \ln(2m + x)/\ln 2$ and fractal dimension $d_B = \ln(2m + x)/\ln 3$.

Figure 3(a) shows the results of the RG flow applied to the fractal model network with $n = 6$, $m = 2$, $x = 1$ with $d_B = 1.46$ for various long-range exponents α. Starting from a pure fractal topology, we pick a node and add a random connection to another node at distance r according to the probability $p(r) = Ar^{-\alpha}$ when $r > 1$ (in our results we repeat this process for 10% of the nodes in the network.) The renormalization is performed numerically using the box-covering algorithm called MEMB in Ref. [11]. Notice that the MEMB algorithm leads to networks that are smaller than the original, and therefore few points are obtained in the plot of $z_b - z_0$ vs x_b. To overcome this problem and obtain better resolution, we take advantage of the self-similar aspect of the network and perform a "partial renormalization," in which parts of the network are subsequently renormalized into supernodes. We follow the behavior of z_b in the RG flow for a given α. For $s < 1$, the average degree follows a power law with exponent $\lambda = 1$ as in Eq. (8). When $s > 1$, the exponent follows the theoretical prediction Eq. (8), $\lambda = 2 - s$. Figure 3(b) shows a very close comparison with theory indicating the transition between the stable region and the unstable region and the optimal navigability point. In Fig. 3(c), we show the dependence of $z_b - z_0$ for different values of N_0. When b is large, finite size effects become evident and the average degree of the renormalized network deviates from the expected power-law of Eq. (7).

An important point readily emerges form the analysis of Eq. (8) when $s = 1$ ($\alpha = d_B$) within the unstable phase as shown in Fig. 2(a). Notice that $s = 1$ coincides with the optimal point of decentralized navigability of Kleinberg

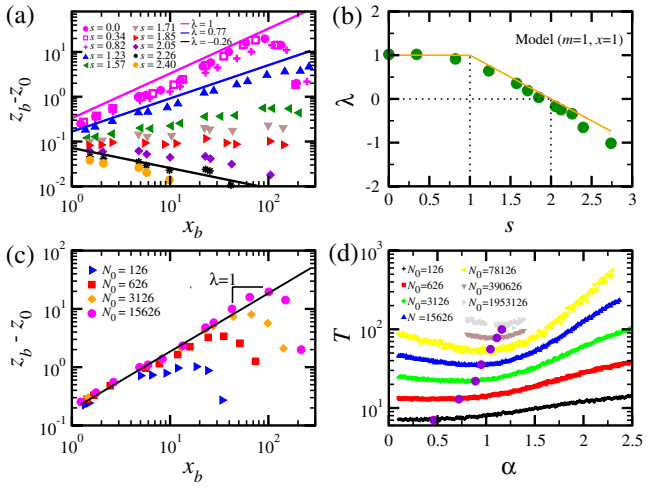

FIG. 3 (color online). Renormalization applied to the fractal model. (a) Average degree of the renormalized network versus x_b for the fractal model with $n = 6$, $m = 2$, $x = 1$. (b) Values of λ obtained from Fig. 3(a) (green data points) and the prediction of the RG from Eq. (7) (solid line). (c) Finite size effects in $z_b - z_0$. (d) Navigation time $T(\alpha)$ for the fractal network model. Circles show the minimum value.

[9] for lattices with fractal dimension d_B [10], and therefore these results could be seen as a plausible extension of the results in Refs. [9,10] for scale-free complex networks. We test this by measuring numerically the average time, $T(\alpha)$, for a message to be delivered from a source node to a target node along the links of the network. It is important to notice that since scale-free networks are not embedded in any euclidean space, one cannot directly apply the decentralized algorithm as introduced by Kleinberg. In the case of scale-free networks, we allow for the message holder to have information on the distance between any node and the target in the fractal background G_0, plus his own shortcuts, but not on (their) the other long-range shortcuts that exists in G'. In Fig. 3(c), we show simulation results for $T(\alpha)$ versus α for the fractal model with $m = 2$, $x = 1$ and for different values of system size N_0. We find that the value $\alpha_c(N_0)$ corresponding to the minimum delivery time for a given N_0 slowly converges to the critical value $\alpha_c(N_0) \to \alpha_c = d_B = 1.46$ as $N_0 \to \infty$, implying a navigability transition at $s = 1$ as predicted by the RG analysis.

An advantage of the RG approach is that it allows for a measurement of the type of shortcuts present in real-world networks. Previously in this Letter, we started with a pure fractal structure G_0 to which shortcuts were added, generating network G', and analyze the stability of G' under the RG procedure. We now switch to the study of real-world networks where we tackle the inverse problem. The real-world networks we examine are known to have an underlying fractal structure since the measurement of N_b versus b leads to a power-law relation [3] [see Fig. 1(b)]. However, these real-world networks already present shortcuts overlaying the fractal structure, and therefore rather than a pure power-law, the scaling shows a cutoff at large b,

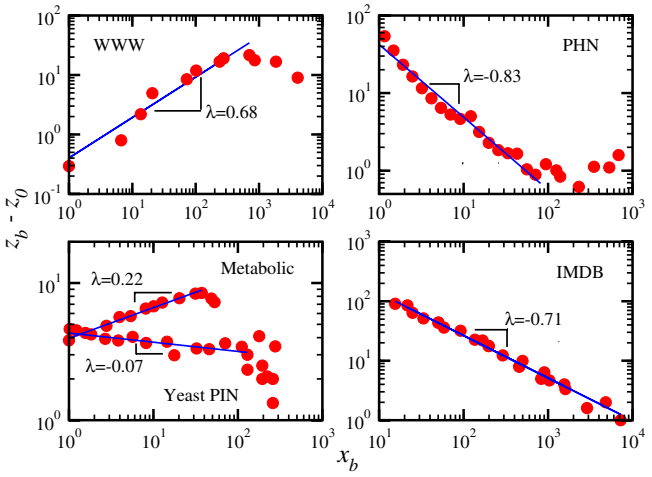

FIG. 4 (color online). Average degree of the renormalized network versus $x_b \equiv N_0/N_b = b^{d_B}$ for the studied samples.

like G' in Fig. 1(b). Therefore, these networks are composed by a fractal underlying structure, analogous to G_0, with some shortcuts generating the network G'. The question we want to answer here is, what is the α exponent of the shortcuts overlaying the fractal network? Since one cannot obtain the value of α directly from the data, we infer its value by treating the real-world network as the network G' and measuring directly the value of λ using the RG flow.

In Fig. 4, we show the results of the RG flow to a sample of the WWW [2], a protein homology network [12], the metabolic network of *E. coli* [13], a yeast protein interaction network [14], and the coacting network of IMDB (we use only the "adult" part of IMDB, not the full database as in [3]) that have been found to exhibit fractal topologies [3]. Table I shows a summary of the exponents for real-world networks. For instance, we find that while the WWW exhibits fractal scaling in N_b [3], it also presents enough shortcuts that its structure belongs to the unstable phase. Thus, the WWW is fractal up to a given length scale, and then it crosses over to small-world behavior at large scales [N_b presents an exponential cutoff at large b, Fig. 1(b)]. The RG determines the crossover scale such that under enough RG steps, the WWW finally becomes a complete graph. Thus, the renormalization allows us to conceptualize the apparent discordance between small-world and fractal properties. Also, due to the its proximity to the $\alpha = d_B$ point, the WWW is sufficiently randomized to give a topology close to optimal information flow. On the contrary, the biological networks PHN and PIN, and the social network of coacting belong to the stable phase indicating that the shortcuts are minimal (the metabolic network is unstable but close to the transition point). The biological networks display a modular deterministic structure shaped by evolution which exhibit pure fractal character that may be seen as a means of protection, preservation, and conservation.

TABLE I. Exponents obtained for the real-world networks.

Network	d_B	λ (Fig. 4)	s from Eq. (8)	phase
WWW	4.1	0.68	1.32	unstable
Metabolic	3.5	0.22	1.78	unstable
PIN	2.2	−0.07	2.07	stable
IMDB	3.5	−0.71	2.71	stable
PHN	2.5	−0.83	2.83	stable

In summary, the RG approach finds the type of shortcuts in a given network and determines the location of a network in the space of configurations. When the exponent of the shortcuts is $\alpha > 2d_B$, the network structure belongs to the stable phase, where RG exhibits a fixed point consisting of a pure fractal network in the space of configurations. On the other hand, when $\alpha < 2d_B$, the network is in the unstable phase where shortcuts become dominant, changing dramatically the global distance between nodes, and leading to a small-world network at large scales.

We thank L. Gallos, S. Havlin, C. Briscoe, and B. Brujic for fruitful discussions. This work was supported by NSF Grants No. SES-0624116 and No. EF-0827508.

[1] P. Erdős and A. Rényi, Publ. Math. Inst. Hung. Acad. Sci. **5**, 17 (1960); D. Watts and S. Strogatz, Nature (London) **393**, 440 (1998).
[2] R. Albert, H. Jeong, and A.-L. Barabási, Nature (London) **401**, 130 (1999).
[3] C. Song, S. Havlin, and H. A. Makse, Nature (London) **433**, 392 (2005).
[4] K. I. Goh, G. Salvi, B. Kahng, and D. Kim, Phys. Rev. Lett. **96**, 018701 (2006).
[5] C. Song, S. Havlin, and H. A. Makse, Nature Phys. **2**, 275 (2006).
[6] J. S. Kim *et al.*, Phys. Rev. E **75**, 016110 (2007); F. Radicchi, J. J. Ramasco, A. Barrat, and S. Fortunato, Phys. Rev. Lett. **101**, 148701 (2008).
[7] L. P. Kadanoff, *Statistical Physics: Static, Dynamics and Renormalization* (World Scientific, Singapore, 2000).
[8] I. Benjamini and N. Berger, Random Struct. Algorithms **19**, 102 (2001).
[9] J. Kleinberg, Nature (London) **406**, 845 (2000).
[10] M. R. Roberson and D. ben-Avraham, Phys. Rev. E **74**, 017101 (2006).
[11] C. Song, L. K. Gallos, S. Havlin, and H. A. Makse, J. Stat. Mech. (2007), P03006.
[12] R. Arnold *et al.*, Bioinformatics **21**, ii42 (2005).
[13] E. Almaas, B. Kovacs, T. Vicsek, Z. N. Oltvai, and A.-L. Barabasi, Nature (London) **427**, 839 (2004).
[14] J.-D. J. Han *et al.*, Nature (London) **430**, 88 (2004).